NOTES AND CORRESPONDENCE

On the Establishment of the Seasonal Pycnocline in the Middle Atlantic Bight*

DAVID C. CHAPMAN AND GLEN GAWARKIEWICZ

Woods Hole Oceanographic Institution, Woods Hole, Massachusetts

18 November 1992 and 5 March 1993

ABSTRACT

Each year the hydrography of the Middle Atlantic Bight changes dramatically from winter conditions with strong horizontal gradients of temperature, salinity, and density at the shelf break separating shelf and slope waters to the summer stratification with a sharp pycnocline at about 20-m depth across both the shelf and slope and weak horizontal density gradients. We use a simple one-dimensional diffusion model to demonstrate that this change could result from a uniform surface heating provided that the nonlinearity of the equation of state is taken into account.

1. Introduction

Late each spring the hydrographic structure of the Middle Atlantic Bight (MAB) undergoes a dramatic transformation from winter stratification to summer stratification (e.g., Bigelow 1933; Bigelow and Sears 1935; Beardsley et al. 1985; Burrage and Garvine 1988; Houghton et al. 1988). During the winter, the water column over the shelf and the upper slope is nearly vertically homogeneous in both temperature and salinity (Fig. 1, left panels). Horizontal gradients dominate and are quite strong near the shelf edge where the fresher, colder shelf water meets the saltier, warmer slope water. The result is a sharp shelf break front in both temperature and salinity. (The temperature and salinity have compensating effects on the density field, but the shelf water is always less dense than the slope water.) In contrast, the summer hydrography exhibits strong vertical gradients over the shelf and slope, especially associated with the seasonal thermocline at roughly 20-m depth (Fig. 1; right panels). Remnants of the strong winter horizontal gradients persist in the temperature and salinity fields, particularly near the bottom, but the density field now exhibits a sharp pycnocline (coincident with the seasonal thermocline) in which nearly horizontal isopycnals connect the shelf and slope waters, leaving little evidence of a cross-frontal density difference. [Numerous examples of these changes may be found in Lyne and Csanady (1984).]

* Woods Hole Oceanographic Institution Contribution No. 8208.

Corresponding author address: Dr. David C. Chapman, Woods Hole Oceanographic Institution, Woods Hole, MA 02543.

The process by which the hydrographic structure changes from the winter to the summer configuration has not been successfully described in detail. The standard qualitative explanation is that solar heating in summer warms the near-surface waters while reduced wind forcing limits the vertical mixing, together leading to a sharp, shallow thermocline. Increased local freshwater runoff slightly alters the salinity distribution, primarily near the coast (e.g., Houghton and Marra 1983; Beardsley et al. 1985; Burrage and Garvine 1988; Houghton et al. 1988).

Although this explanation sounds reasonable, it is not obvious that it can account for the seasonal changes. For example, consider the extremely simple case of a spatially uniform surface *density* flux, attributable to solar heating, applied to the winter density field in Fig. 1. Considering only diffusive processes and ignoring advection (i.e., currents), this density flux cannot form the summer density field in Fig. 1 because there is no way of altering the horizontal density gradients. That is, the density at a given depth would change by the same amount at all horizontal locations, leaving the original horizontal gradients intact.

One possible solution to this dilemma might be to invoke a spatially varying density flux due to spatial variations in the heat and salt fluxes (Aikman 1984; Aikman and Posmentier 1985). However, the density fluxes over the shelf and slope estimated by Aikman (1984) increased the density difference between the upper layers during summer (cf. Fig. 4c of Aikman and Posmentier 1985), which appears to conflict with recent observations (e.g., Beardsley et al. 1985; Burrage and Garvine 1988; Houghton et al. 1988).

As a simpler alternative explanation, we propose that the reduced horizontal density gradients across the shelf

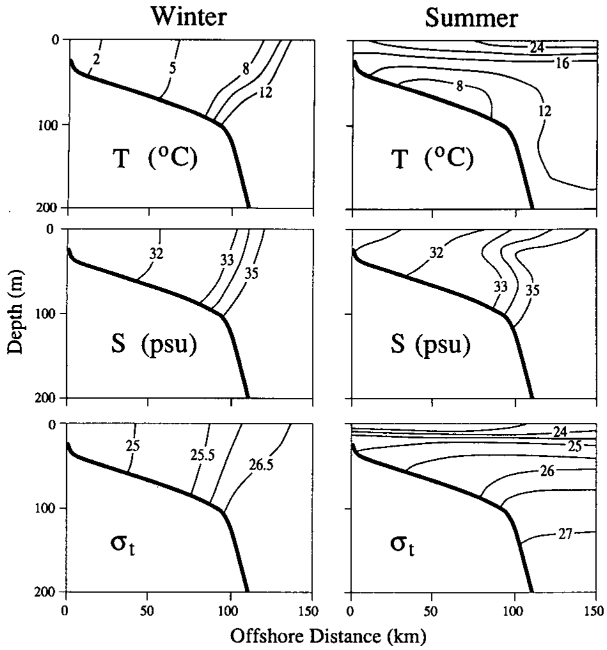

FIG. 1. Schematic of typical (left panels) winter and (right panels) summer hydrography in the Middle Atlantic Bight, showing (upper) temperature, (middle) salinity, and (lower) density fields.

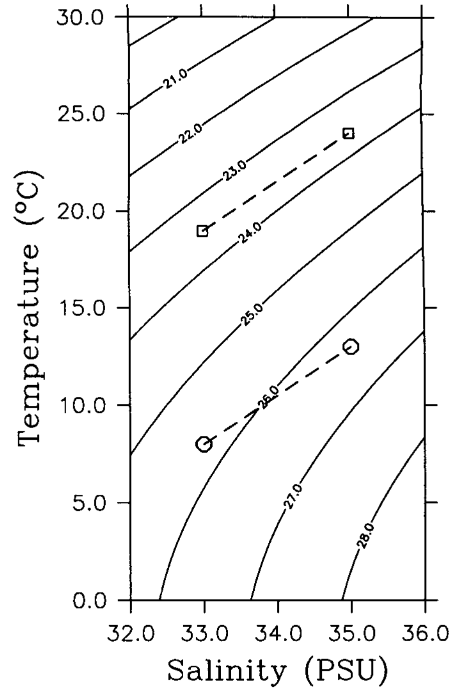

FIG. 3. Temperature–salinity diagram showing typical properties of water at the surface on either side of the shelf break front for (circles) winter and (squares) summer. The shelf water is colder and fresher than the slope water. Curved lines are density contours in σ_t units.

break front in summer may be largely accounted for by the often neglected nonlinearity of the equation of state. To illustrate, consider typical seasonal variations of near-surface water parcels on opposite sides of the shelf break front. In winter, the front separates shelf water at roughly $T \approx 8°C$ and $S \approx 33$ psu from slope water at roughly $T \approx 13°C$ and $S \approx 35$ psu. The density difference between the two parcels, using the nonlinear equation of state (Millero et al. 1980), is $\Delta\rho = 0.68$ kg m^{-3}. As summer approaches, surface waters become warmer but the horizontal temperature gradients remain. This is shown in Fig. 2 where we have plotted the annual temperature cycle for surface waters at stations on the shelf (40°40′N, 70°30′W) and over the slope (39°50′N, 70°30′W) based on the extensive MARMAP surveys (Mountain 1989). The temperature difference between the two stations (solid curve) is always positive, varying from about 2°C in spring to 5°C in summer. The seasonal variation in salinity at these locations is small and is dominated by interannual variability (Mountain 1991; Manning and Holzworth 1990), so for the purposes of this illustration, we approximate the summer conditions by simply increasing the winter temperature of each water parcel by 11°C while holding the salinity fixed. Thus, the summer shelf water parcel has $T \approx 19°C$ and $S \approx 33$ psu, while the slope water parcel has $T \approx 24°C$ and $S \approx 35$ psu.[1] The corresponding summer density difference is $\Delta\rho = 0.14$ kg m^{-3}, substantially reduced from the winter density difference.

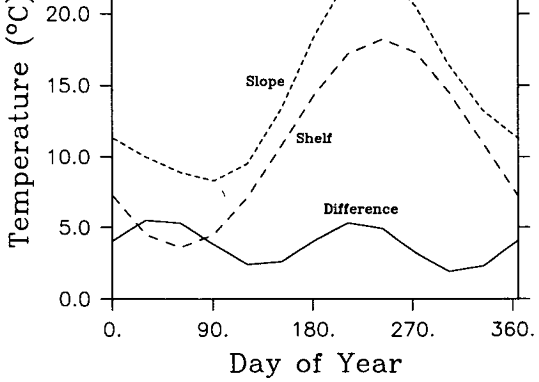

FIG. 2. Annual cycle of surface temperature for stations over the slope (short dashed curve) and on the shelf (long dashed curve). The solid curve is the temperature difference between the two stations.

Figure 3 graphically shows the importance of the nonlinear equation of state for the example described above. The circles on the T–S diagram represent the winter water parcels. The line connecting them clearly

[1] The persistence of a 5° cross-frontal temperature difference is consistent with typical conditions in the northern MAB (e.g., Fig. 4 of Houghton et al. 1988) but is atypical of the southern MAB where the cross-frontal temperature difference is greatly reduced in summer.

crosses the $\sigma_t = 26$ contour at a substantial angle, indicating a significant density difference. The squares represent the summer water parcels, which are 11°C warmer than the winter parcels. The line connecting the summer parcels is nearly parallel to the $\sigma_t = 24$ contour, indicating a reduced density difference. Therefore, this example shows that a spatially *uniform* surface heat flux can produce nearly equal densities on both sides of the shelf break front despite the continued presence of horizontal gradients in both salinity and temperature, simply because the equation of state is nonlinear.

The effect of this nonlinear behavior on the spatial structure of the density field is demonstrated more completely with a simple example in section 2. The relevance of the results to the MAB is discussed in section 3.

2. A simple example

We demonstrate the importance of the nonlinearity of the equation of state on the spatial structure of the density field with a fairly simple calculation, which builds on the scenario described in the Introduction. Consider a flat-bottom shelf of depth $H = 100$ m that contains only horizontal variations in temperature and salinity given by

$$T(°\mathrm{C}) = 10.5 + 2.5\tanh[(x - L)/2] \quad (1)$$

$$S(\mathrm{psu}) = 34 + \tanh[(x - L)/2], \quad (2)$$

where L is the horizontal scale of the shelf (Fig. 4). The maximum horizontal gradient occurs at $x = L$. The water to the left of the front represents winter shelf water, while the water to the right of the front represents winter slope water (i.e., the circles in Fig. 3). The third panel shows the density field (σ_t units) computed using a linear form of the equation of state,

$$\rho(\mathrm{kg\ m^{-3}}) = 26.312 - 0.175(T - 10.5) + 0.779(S - 34), \quad (3)$$

while the lowest panel is the density field computed using the nonlinear equation of state (Millero et al. 1980). The two initial density fields are only slightly different.

We apply a uniform constant heating at the surface of the temperature field in Fig. 4 and assume that vertical mixing is the only process taking place. That is, we assume that there is no horizontal mixing and there are no currents. These are indeed drastic assumptions that remove all horizontal dependence from the model—a major departure from reality. However, they represent the extreme condition in which the seasonal changes cannot be caused by any horizontal variations in the forcing or the response and, as such, serve to isolate the changes due solely to the nonlinearity of the equation of state, which is our objective. With these simplifications, the temperature field is described by

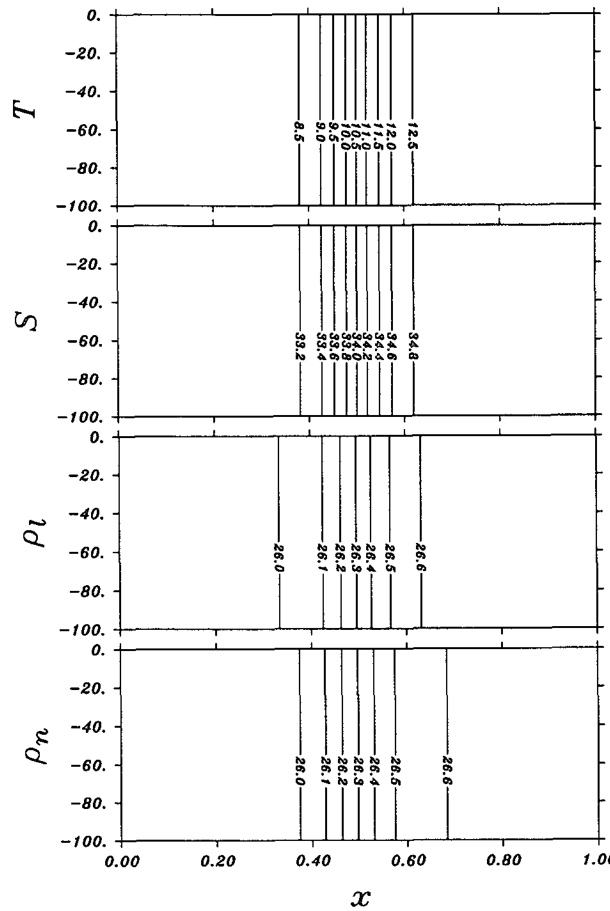

FIG. 4. Initial (upper) temperature and (second) salinity fields used in the one-dimensional diffusion model. The lower two panels show the corresponding initial density fields using the (third) linear and (lower) nonlinear equations of state. The cross-shelf distance has been scaled by $2L$.

$$\frac{\partial T}{\partial t} = \frac{\partial}{\partial z}\left(\kappa(z)\frac{\partial T}{\partial z}\right), \quad (4)$$

where $\kappa(z)$ is the vertical diffusion coefficient, z is depth, and t is time. Given the initial temperature field, a surface heat flux, and κ, (4) can be integrated numerically at many x locations to follow the evolution of the temperature field.

Figure 5 shows the temperature field (upper panel) after 180 days of heating by a surface heat flux of 2.5×10^{-5} °C m s^{-1} with $\kappa = 0.0002$ m^2 s^{-1}. This heat flux corresponds to a typical summer solar heating of 100 W m^{-2}. The temperature has increased uniformly at the surface and the heat has diffused downward, warming the entire water column to some extent, but the horizontal temperature gradients are still large across the frontal region. By assumption, the salinity field is unchanged. The third panel shows the density field computed using the linear equation of state. The isopycnals are clearly horizontal *away* from the frontal

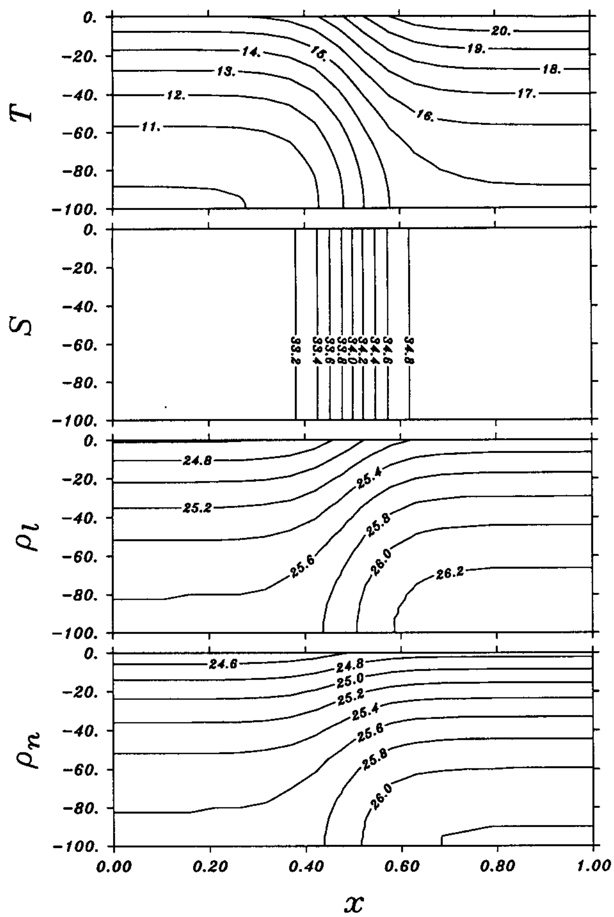

FIG. 5. As in Fig. 4 but after 180 days of heating by a surface heat flux of 2.5×10^{-5} °C m s^{-1}. The diffusion coefficient is constant at $\kappa = 0.0002$ m^2 s^{-1}.

region, but the horizontal density *gradients* are unchanged from the initial state (Fig. 4), as they must be in a completely linear calculation. Only two isopycnals connect the two sides of the frontal region, and then at quite different depths on each side.

The lowest panel of Fig. 5 shows the density field computed from the same temperature and salinity fields but now using the nonlinear equation of state. Note that the horizontal density gradients are greatly reduced across the frontal region and that several nearly level isopycnals connect the two sides of the front, despite the presence of strong horizontal gradients in both temperature and salinity! There is still a reasonably strong horizontal density gradient near the bottom, consistent with observations. Basically, the increased change in temperature near the surface has made the temperature more important in determining the density in the upper part of the water column than it was for the winter conditions.

The assumption of a constant vertical mixing coefficient is extreme and ignores the anticipated effect of the shallow mixed layer. In the ocean we expect vertical mixing to be largest within the surface mixed layer and reduced at depth. To include this effect (rather crudely), we have repeated the previous calculation using a depth-dependent mixing coefficient of the form

$$\kappa(\mathrm{m^2\,s^{-1}}) = 5 \times 10^{-5} + 4.75 \times 10^{-4}\{1 + \tanh[(z + 10)/5]\}. \quad (5)$$

This mixing coefficient changes smoothly from a maximum of 0.001 m^2 s^{-1} near the surface to a minimum of 5×10^{-5} m^2 s^{-1} at depth, with the variation occurring fairly rapidly at $z = -10$ m. That is, mixing above 10-m depth is strong, while mixing below 10 m is weak.

After applying the same heating at the surface for 180 days, the resulting temperature and density fields are shown in Fig. 6, using the same format as in Fig. 5. This choice of mixing coefficient basically traps the heat near the surface, so the temperature field now exhibits a noticeable, though somewhat diffuse, thermocline between 20 and 40 m. This is reflected in both

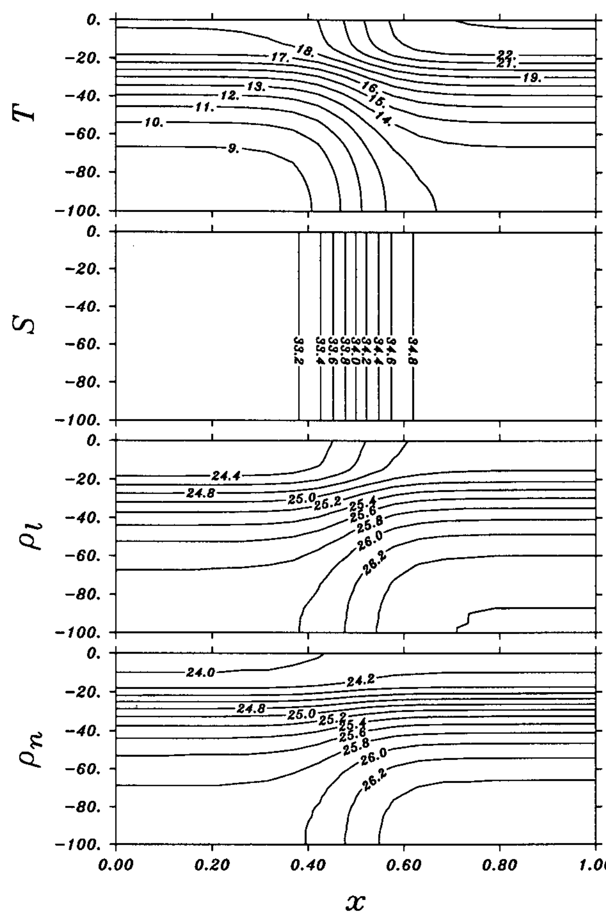

FIG. 6. As in Fig. 5 but using the vertically varying diffusion coefficient given by (5); that is, mixing is strong (weak) above (below) 10-m depth.

density fields as well. However, the density field computed with the linear equation of state (third panel) still contains the original horizontal gradients across the frontal region, while the density field computed with the nonlinear equation of state (lowest panel) exhibits greatly reduced horizontal gradients across the frontal region in and above the pycnocline. The structure of the horizontal density gradients is shown in Fig. 7. The horizontal density gradients are relatively unchanged below the pycnocline in the nonlinear case because the temperature has not changed appreciably. As in Fig. 5, the water masses on both sides of the frontal region are connected by nearly level isopycnals in the nonlinear case (Fig. 6), despite the continued presence of strong horizontal gradients in both temperature and salinity.

3. Discussion

The simple example presented in the previous section demonstrates that the nonlinearity of the equation of state can have profound effects on the density field for the range of temperatures and salinities characteristic of the MAB. The results suggest that the frequently observed winter-to-summer seasonal changes in the density field of the MAB may, to a large extent, simply reflect this nonlinearity. Complicated dynamics and forcing may not be required to explain much of the seasonal change.

If this reasoning is correct, then some important implications follow. For example, the continued presence of a relatively constant salinity difference across the shelf break front is crucial because it allows the increase in the relative importance of temperature in determining the near-surface density during summer. This can be seen by examining Fig. 3. If the salinity gradients change significantly, then the density gradients across the front may not weaken during summer. This, in turn, implies that the basic cross-frontal salinity difference cannot be a seasonal feature associated with local freshwater runoff but instead must be established upstream along the shelf. This is consistent with recent ideas about the origin of the shelf water in the MAB (Chapman and Beardsley 1989). Further support for the unlikelihood of a locally formed salinity difference comes from the study of Chapman and Lentz (1992), who showed that a coastal freshwater source does not readily fill the shelf with fresh water. Taken together, these imply that the shelf break front in the MAB is probably established well upstream where the difference between shelf and slope water properties is introduced, perhaps at Hudson Strait. The seasonal variations in temperature (and, hence, density) would then be primarily a local phenomenon.

Another interesting point is that this response may be peculiar to midlatitude shelves and not apply to shelf break fronts at high latitudes. For instance, the shelf break front along the east Greenland coast would not behave the same way in the presence of the same heating. There, the density is dominated by the salinity, so seasonal changes in the temperature would not introduce appreciable changes in the density field even using the nonlinear equation of state. However, midlatitude shelf break fronts in other locations may be subject to the same effects of the nonlinearity of the equation of state as described here.

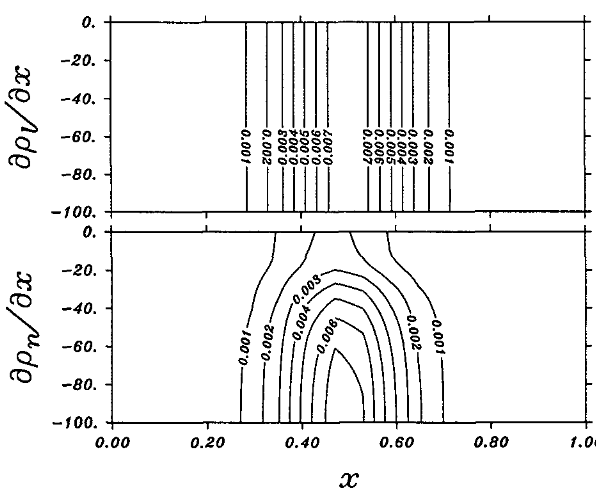

FIG. 7. Contours of horizontal density gradient computed from the density fields in Fig. 6. Upper and lower panels are the linear and nonlinear cases, respectively. In the nonlinear case, the gradient is greatly reduced within and above the pycnocline.

Acknowledgments. We thank Dave Mountain for sharing his TEMPEST software. Helpful comments from two anonymous reviewers are greatly appreciated. Financial support was provided by the National Science Foundation under Grants OCE88-16015 (DCC) and OCE90-16893 (GG). The latter grant is part of the U.S. Global Ocean Ecosystems Dynamics (GLOBEC) program.

REFERENCES

Aikman, F., III, 1984: Pycnocline development and its consequences in the Middle Atlantic Bight. *J. Geophys. Res.*, **89**, 685–694.

——, and E. S. Posmentier, 1985: Stratification and shelf-slope interaction in the Middle Atlantic Bight: A numerical study. *J. Geophys. Res.*, **90**, 4895–4905.

Beardsley, R. C., D. C. Chapman, K. H. Brink, S. R. Ramp, and R. Schlitz, 1985: The Nantucket Shoals Flux Experiment (NSFE79). Part 1: A basic description of the current and temperature variability. *J. Phys. Oceanogr.*, **15**, 713–748.

Bigelow, H. B., 1933: Studies of the waters on the continental shelf, Cape Cod to Chesapeake Bay. 1: The cycle of temperature. *Papers Phys. Oceanogr. Meteor.*, **2**(4), 135 pp.

——, and M. Sears, 1935: Studies of the waters on the continental shelf, Cape Cod to Chesapeake Bay. 2: Salinity. *Papers Phys. Oceanogr. Meteor.*, **4**(1), 94 pp.

Burrage, D. M., and R. W. Garvine, 1988: Summertime hydrography at the shelfbreak front in the Middle Atlantic Bight. *J. Phys. Oceanogr.*, **18,** 1309–1319.

Chapman, D. C., and R. C. Beardsley, 1989: On the origin of shelf water in the Middle Atlantic Bight. *J. Phys. Oceanogr.*, **19,** 384–391.

——, and S. J. Lentz, 1992: Trapping of a coastal density front by the bottom boundary layer. *J. Phys. Oceanogr.*, submitted.

Houghton, R. W., and J. Marra, 1983: Physical/biological structure and exchange across the thermohaline shelf/slope front in the New York Bight. *J. Geophys. Res.*, **88,** 4467–4481.

——, F. Aikman III, and H. W. Ou, 1988: Shelf–slope frontal structure and cross-shelf exchange at the New England shelf-break. *Contin. Shelf Res.*, **8,** 687–710.

Lyne, V. D., and G. T. Csanady, 1984: A compilation and description of hydrographic transects of the Mid-Atlantic Bight shelf-break front. Woods Hole Oceanographic Institution Tech. Rep. 84-19, 290 pp.

Manning, J., 1991: Middle Atlantic Bight salinity: Interannual variability. *Contin. Shelf Res.*, **11,** 123–137.

——, and T. J. Holzworth, 1990: Description of the oceanographic conditions on the northeast continental shelf, 1977–1985. Laboratory reference document 90-04, Northeast Fisheries Center, Woods Hole, MA, 373 pp.

Millero, F. J., C.-T. Chen, A. Bradshaw, and K. Schleicher, 1980: A new high pressure equation of state for seawater. *Deep-Sea Res.*, **27,** 255–264.

Mountain, D. G., 1989: TEMPEST: A computer program for estimating temperature on the northeast continental shelf. Laboratory reference document 89-02, Northeast Fisheries Center, Woods Hole, MA, 8 pp.

——, 1991: The volume of shelf water in the Middle Atlantic Bight: Seasonal and interannual variability, 1977–1987. *Contin. Shelf Res.*, **11,** 251–267.